Published in final edited form as:
*Opt Express*. 2008 October 13; 16(21): 16552–16560.

# Characterization of FBG sensor interrogation based on a FDML wavelength swept laser

**Eun Joo Jung**[1,2], **Chang-Seok Kim**[1], **Myung Yung Jeong**[1], **Moon Ki Kim**[3], **Min Yong Jeon**[4], **Woonggyu Jung**[2,5], and **Zhongping Chen**[2,5]

[1]Department of Nanosystem Engineering, Pusan National University, Busan, Korea 609-735

[2]Beckman Laser Institute, University of California, Irvine, Irvine, California 92612

[3]School of Mechanical Engineering, Sungkyunkwan University, 300 Suwon, Korea 440-746

[4]Department of Physics, Chung Nam National University, Daejeon, Korea 305-764

[5]Department of Biomedical Engineering, University of California, Irvine, Irvine, California 92612

## Abstract

In this study, we develop an ultra-fast fiber Bragg grating sensor system that is based on the Fourier domain mode-locked (FDML) swept laser. A FDML wavelength swept laser has many advantages compared to the conventional wavelength swept laser source, such as high-speed interrogation, narrow spectral sensitivity, and high phase stability. The newly developed FDML wavelength swept laser shows a superior performance of a high scan rate of 31.3 kHz and a broad scan range of over 70 nm simultaneously. The performance of the grating sensor interrogating system using a FDML wavelength swept laser is characterized in both static and dynamic strain responses.

## 1. Introduction

The fiber Bragg gratings (FBGs) sensor system has been widely used for structural health monitoring in civil infrastructures, aerospace, wind energy, and maritime areas. It has many advantages over other electrical and optical strain sensors, such as electromagnetic interference (EMI) resistance, long distance sensing, wavelength selectivity and environmental endurance, and reduced size [1]. To interrogate the peak movement of FBGs, various wavelength detection techniques have been reported based on a passive optical filter or interferometer [2–8]. For the high speed and high sensitivity monitoring of multiple FBG sensors, wavelength-swept fiber lasers have been introduced for the development of optical source interrogation [9–11]. When a central lasing peak is repeatedly swept over the spectrum range of remote FBGs sensors, reflected signals from FBGs arrays are simultaneously detected in the single detector. Reflected optical signals consist of a series of pulses in the time domain. Even though this technique provides improved performance to the passive interrogation methods, the maximum speed of the conventional wavelength swept laser source was physically limited to the kHz regime because of the cavity round-trip and energy building up of the optical gain [12].

The novel development of a wavelength swept laser source with speeds over 10 kHz is strongly expected to broaden the range of applications of the FBG sensor systems, such as monitoring the real-time strain of the high-speed dynamic fluidic sloshing pressure in a



Corresponding authors: myjeong@pusan.ac.kr, z2chen@uci.edu.

liquefied natural gas (LNG) carrier ship [13–17]. Since electric-type sensors do not work properly in a cryogenic temperature environment (< −160 °C), FBG sensors have been expected to become an ideal dielectric device for massive LNG carrier ships but their maximum interrogating speed has been limited to the kHz regime [9–11]. In this study, we developed an ultra-fast 31.3 kHz FBG sensor system that operates in the 1.5 μm wavelength regions using Fourier domain mode-locked (FDML) swept laser technology. Given the rapidly increasing global demand for oil and natural gas, this novel advancement in ultra-fast interrogation may be useful for the real-time strain monitoring in the hazardous cargo containment of LNG tankers, in addition to the ideal nature of explosive-free, multi-point telemetry and low-temperature performance of the FBG sensor [14–15].

The FDML technology has recently been developed around the 1.3 μm biomedical optics field for the high speed *in vivo* imaging of optical coherence tomography (OCT) [18–21]. In the FDML wavelength swept laser, a long delay line fiber is incorporated into the laser ring cavity and the tunable optical bandpass filter is driven at a time period that is either matched to the round-trip time of the cavity or its harmonics. Light from the previous round-trip is coupled back to the gain medium and an entire wavelength sweep is optically stored within the laser cavity. Unlike the conventional wavelength swept laser source, the FDML wavelength swept laser does not need to build up its lasing energy from repeated spontaneous emissions. Thus, the superior performances of more than hundred kHz sweeping rate and high phase stability have been reported for the 1.3 μm wavelength region in the OCT *in vivo* imaging fields [19][20] and other ultra-fast spectroscopic analysis applications [22].

## 2. Experimental setup

### 2.1 Comparison of the conventional wavelength swept laser and FDML wavelength swept laser

Figure 1 shows the schematic configurations of the conventional wavelength swept laser and the FDML wavelength swept laser. Both lasers use a ring cavity and are composed of two isolators for a unidirectional ring configuration, an output coupler, a polarization controller (PC), a fiber Fabry-Perot tunable filter (FFP-TF produced by Lambda Quest Co.) and a semiconductor optical amplifier (SOA produced by Covega Co.). In the FDML wavelength swept laser, a delayed fiber of several kilometers is inserted to match the scanning time of a tunable filter with the round-trip time of the cavity. Since we hold two kinds of optical fiber spools, 6.7 km and 11.5 km in our laboratory, we can operate the laser at the fastest sweeping rate of 31.3 kHz using 6.7 km fiber in this study. For the comparison reason, a longer fiber length of 11.5 km was necessary for operation at 18 kHz. The FFP-TF has a linewidth of 0.25 nm and a free spectral range of 150 nm. This filter was modulated with a sinusoidal waveform to produce a wavelength sweep in this spectral region. The SOA has a saturation output power of 2.3 mW and a polarization sensitivity of ~0.5 dB. The spontaneous emission spectrum of this amplifier had a center wavelength at ~1540 nm with a full width at half maximum (FWHM) of 50 nm. The maximum available current was 600 mA, therefore all the experimental results presented here was driven by a 300 mA current source, providing a small signal gain of 20 dB at 1550 nm.

For comparison purposes, three spectra obtained from the conventional wavelength swept laser output were plotted together in the linear scale, as shown in Fig. 2. These spectra were measured in the peak hold mode of the optical spectrum analyzer (OSA). For the sweeping rates of 0.1 kHz, 1 kHz and 10 kHz, the average power of each optical source was measured to be 0.39 mW, 0.21 mW and 0.11 mW, respectively. At the sweeping rate of 0.1 kHz, the edge-to-edge scanning range was approximately 97 nm, from 1479 nm to 1576 nm, and the corresponding 3 dB sweeping bandwidth of the peak hold lasing spectrum was

approximately 70 nm. However, at increasing sweeping rates, the output power of the laser dramatically decreased and the spectral shape at 10 kHz was seriously distorted relative to 0.1 kHz.

Three transient intensity profiles, corresponding to the above sweeping operations, are temporally presented in Fig. 3. As with Fig. 2, the amplitudes of the temporal transient intensity profiles significantly decreased with increasing sweeping rates from 0.1 kHz to 1 kHz and 10 kHz. It is also worth noting that all of the profiles were asymmetric during the forward scan and backward scan. This intensity asymmetry was attributed to the frequency downshift of nonlinear processes generated in the gain medium of the SOA [23]. It has been suggested that placing a booster amplifier before the position of main SOA. However, the maximum tuning speed was still limited at a frequency region between the saturation limit and the single roundtrip limit in the conventional wavelength swept laser under these conditions [24]. Therefore, this system is still insufficient to detect a dynamic strain response in the kHz range, such as detecting rapid fluidic sloshing pressure variation. In order to overcome the speed limit of the conventional wavelength swept laser, the FDML wavelength swept laser has been developed to interrogate the sensing dynamics of FBGs.

Figure 4(a) shows two spectra of the FDML wavelength swept laser at an 18 kHz and 31.3 kHz sweeping rate. For both cases, the 3 dB sweeping bandwidth of the FDML wavelength swept laser was approximately 70 nm, which was caused by the edge-to-edge scanning range from 1481 nm to 1575 nm. The measured average output power of FDML wavelength swept laser was 0.28 mW and 0.26 mW, respectively. Figure 4(b) shows one of the temporal transient intensity profiles of the FDML wavelength swept laser operated at a 31.3 kHz frequency. Although the scanning rate of FFP-TF was increased, the amplitude of the profiles maintained the same power level and temporal response during forward and backward scanning, unlike the temporal transient intensity profiles of the conventional wavelength swept laser. We can observe that the temporal widths of forward and backward scanning become identical as the sweeping time and roundtrip time of laser are getting closed. It is obvious that the lasing of the FDML wavelength swept laser does not depend on the buildup time from the spontaneous emission of the optical source and the mechanical behavior of tunable filter. When we controlled the physical cavity length of laser ring cavity, the higher scanning speed of the FDML laser can be demonstrated easily. By using the FDML wavelength swept laser at a sweeping rate of 31.3 kHz, the ultra-fast interrogation of the Bragg wavelength shift of the FBG can be experimentally performed.

### 2.2 FBG sensor interrogation system with sensor array

Figure 5 shows the schematic of a FBGs sensor interrogation system using the FDML wavelength swept laser with sweeping rate of 31.3 kHz. The laser output passes a circulator and is coupled into an array of four FBG sensors. The center wavelengths of the four FBGs in the sensor array are 1534.1, 1536.7, 1541.8 and 1549.2 nm, respectively. All of the FBGs displayed a reflectivity of more than 90 % and a narrow 3 dB bandwidth of around 0.2 nm. The reflection signals from FBGs sensors were acquired using a high speed photo-detector with 125 MHz bandwidth (model 1811-FC, New Focus) and a data acquisition board with 100 Msamples/s and 14bit resolution (model NI 5122, National Instruments). By repeating the lasing peak scanning over the spectral range of the four FBGs sensors, we can simultaneously detect the reflected signals, which consist of a series of pulses in the time domain. Since the time intervals in the photo detector and spectral intervals of FBG sensors correspond to each other, the variance of the Bragg wavelength of each FBG sensors can be easily converted to the scanning speed of FDML wavelength swept laser source. In order to find the exact peak points in the time trace of the reflection signals, optimal algorithm of LabVIEW® program was applied to search one position with maximum value in the given operating region. For multiple FBG sensor array, the boundary of defined region was

selected in advance based on the operating wavelength range of each FBG sensor. By repeatedly determining the multiple peak positions over the whole wavelength region, the temporal variations of multiple peaks could be visualized in real time by designed software.

## 3. Experimental result of the sensor array system

### 3.1 Response to static strain

Figure 6(a) shows, in the time domain, a reflection signal from the sensor array with four FBGs. For a direct comparison of the time domain signal and the wavelength domain response in the FBG sensor interrogation system based on the FDML wavelength swept laser, we also measured the reflection spectrum using a static broadband light source (Fig. 6(b)). The reflection response in the wavelength domain was obtained by OSA at a resolution of 0.1 nm. Since the signal was simultaneously measured with the FDML wavelength swept laser at 31.3 kHz, the spectral range from $FBG_1$ to $FBG_4$, 15.1 nm, corresponded to the scanning time range from $\tau 1$ to $\tau 4$, 3.024 μs. As a result, the FDML wavelength swept laser showed a linear relationship with wavelength sweeping because all reflection signals had the exact same interval in both domains. It is suspected that the intensity overshoots in the bottom area near reflection signal of Fig. 6(a) comes from RF bandwidth limitation, but they will not affect to the peak tracking in the given operating region. The effective spectral width of time-domain peaks in Fig. 6(a) looks wider in comparison with the wavelength-domain peaks in Fig. 6(b). It can be explained from the spectral interval of the time-domain signal. If we increase the number of data acquisition per each forward scanning of FFP-TF, which was 1024 points in Fig. 6(a), the spectral interval of the time-domain signal will become much narrower.

Figure 7 depicts a typical response by an applied static strain for one of the FBGs ($\tau 3$). One side of the grating $\tau 3$ was attached on the fixture and the other side of that was fixed on a piezoelectric transducer (PZT) motorizing stage, as shown in Fig. 5. The grating $\tau 3$ was applied with static strain to the unidirectional side. Since the grating $\tau 3$ was mounted tightly by the initial strain, the time delay between $\tau 3$ and $\tau 2$ shows a linear response against the applied static strain. The vertical axis of Fig. 7 indicates the time delay ($\tau 3$-$\tau 2$) variation and the horizontal axis displays the applied strain with a small step of 0.25 mε. The applied strain by displacing a PZT stage is defined by the ratio between the strained length and original length of the FBG sensor. The best-fit slope coefficient for the measured time delay data was determined to be 98.6 ± 2 ns/mε.

The resolution of measurement was also demonstrated for 1000 times repetition of 31.3 kHz operation. The reflection signals from the $FBG_3$ sensor without applied strain were acquired during forward scanning of FFP-TF. By observing the standard deviation of strains on the grating $\tau 3$ during 0.032 s, a root mean square (RMS) was acquired to 2.6 ns using a signal-processing algorithm in LabVIEW® software. This value corresponds to a strain resolution of 26.4 $\mu\varepsilon_{rms}$ and to a spectral resolution of 13 pm [9]. Though the PZT component in FFP-TF has a hysteresis and non-linear response against a linear modulation signal, there have been several techniques to improve the resolution by the Fabry-Perot etalon used for a grid line and a stabilization-controlling unit [8–10].

### 3.2 Response to dynamic strain

To assess the dynamic performance of this FBG sensor system, a modulation signal was also applied to the grating $\tau 3$. Figure 8(a) shows the driving waveform signal that was applied to the PZT stage. A sinusoidal waveform of 100 Hz frequency and 10 V applied voltage was the input signal into the PZT stage. Figure 8(b) shows the corresponding output signals from the FBG sensor interrogation system based on the proposed FDML wavelength swept laser at the sweeping rate of 31.3 kHz. Reflected FBG signals collected by the photo-detector

were effectively digitized using a data acquisition board with a high rate of 100 Msamples/s because the large number of 1024 data set was required during 0.032 ms for each single sweep of 31.3 kHz. Among the 1024 points in the time trace of the reflection signals, the peak point was easily determined using peak search algorithm and the variation of each peak point was repeatedly traced for 1940 times during 62 ms.

From these experiments, it was demonstrated that the applied signal was entirely reinstated in the proposed sensor system. The peak–peak amplitude of the dynamic strain was approximately 636 $\mu\varepsilon$, which matched well with the applied strain conditions. The RMS value of the applied strain was calculated to 197.42 $\mu\varepsilon_{FBG,\ rms}$ from the set of time-interval values obtained using the FBG sensor. The appropriate power spectral density (PSD) Fast Fourier Transform (FFT) spectrum was also monitored for the dynamic strain at 100 Hz as shown in Fig. 9. From this, the signal to noise ratio (SNR) and frequency bandwidth were determined to be 40.53 dB and 12.75 Hz, respectively. Since the RMS value of the strain noise level was easily induced as 1.86 $\mu\varepsilon_{noise,\ rms}$, it was equal to the ratio of the applied strain RMS and the SNR. From the RMS value of the strain noise level and the frequency bandwidth, the strain sensitivity, which is the strain noise level RMS over the square root of the frequency bandwidth, was determined to be 0.52 $\mu\varepsilon_{rms}$/Hz [7,25].

## 4. Conclusion

In summary, we have developed and experimentally demonstrated the capabilities of a novel ultra-fast FBG strain sensor monitoring system based on a FDML wavelength swept laser. The FDML wavelength swept laser displayed a high performance at a 31.3 kHz sweeping rate, an average output power of 0.26 mW, and a wavelength scan range of over 70 nm. Since the sweeping rate simply corresponds to the round trip time, the speed of the system can be easily improved to higher than hundreds kHz by controlling the fiber length in the laser cavity. This laser was then applied to measure the dynamic variation of structural strains using an FBG sensor system. The improved interrogating speeds demonstrated in this study can be useful for various novel ultra-fast sensing applications.

## Acknowledgments

This work was supported by research grants from the National Science Foundation (BES-86924), National Institutes of Health (EB-00293, NCI-91717, RR-01192), and the Air Force Office of Scientific Research (FA9550-04-1-0101), USA. This work was supported by the IT R&D program of MKE/IITA [2008-F-020-01], Korea. Supports from the Beckman Foundation and the second stage of the Brain Korea 21 Project in 2008 are also acknowledged. The FBGs used in the experiments were supplied by FBG Tech Co., Korea.

## References and links

1. Kersey AD, Davis MA, Patrick HJ, LeBlane M, Koo KP, Askins CG, Putnam MA, Friebele EJ. Fiber grating sensors. J Lightwave Technol. 1997; 15:1442–1463.
2. Melle SM, Liu K, Measures RM. A Passive Wavelength Demodulation System for Guided-Wave Bragg Grating Sensors. IEEE Photon Technol Lett. 1992; 4:1539–1541.
3. Kersey AD, Berkoff TA, Morey WW. High-resolution fiber Grating based strain sensor with interferometric wavelength-shift detection. Electron Lett. 1992; 28:236–238.
4. Kersey AD, Berkoff TA, Morey WW. Multiplexed fiber Bragg grating strain-sensor system with a fiber Fabry-Perot wavelength filter. Opt Lett. 1993; 18:33–39.
5. Kim CS, Lee TH, Yu YS, Han YG, Lee SB, Jeong MY. Multi-point interrogation of FBG sensors using cascaded flexible wavelength-division Sagnac loop filters. Opt Express. 2006; 14:8546–8551. [PubMed: 19529233]
6. Chung S, Kim J, Yu BA, Lee B. A fiber Bragg grating sensor demodulation technique using a polarization maintaining fiber loop mirror. IEEE Photon Technol Lett. 2001; 13:1343–1345.

7. Song M, Yin S, Ruffin PB. Fiber Bragg grating strain sensor demodulation with quadrature sampling of a Mach–Zehnder interferometer. Appl Opt. 2000; 39:1106–1111. [PubMed: 18337990]
8. Bang H-J, Jun S-M, Kim C-G. Stabilized interrogation and multiplexing techniques for fibre Bragg grating vibration sensors. Meas Sci Technol. 2005; 16:813–820.
9. Yun SH, Richardson DJ, Kim BY. Interrogation of fiber grating sensor arrays with a wavelength-swept fiber laser. Opt Lett. 1998; 23:843–845. [PubMed: 18087360]
10. Ryu C-Y, Hong C-S. Development of fiber Bragg grating sensor system using wavelength-swept fiber laser. Smart Mater Struct. 2002; 11:468–473.
11. Wang Y, Cui Y, Yun B. A Fiber Bragg Grating Sensor System for Simultaneously Static and Dynamic Measurements With a Wavelength-Swept Fiber Laser. IEEE Photon Technol Lett. 2006; 18:1539–1541.
12. Lee S-W, Kim C-S, Kim B-M. External-line cavity wavelength-swept source at 850 nm for optical coherence tomography. IEEE Photon Technol Lett. 2007; 19:176–178.
13. Hongo A, Kojima S, Komatsuzaki S. Applications of fiber Bragg grating sensors and high-speed interrogation techniques. Struct Control Health Monit. 2005; 12:269–282.
14. Kim DG, Yoo W, Swinehart P, Jiang B, Haber T, Mendez A. Development of an FBG-Based Low Temperature Measurement System for Cargo Containment of LNG Tankers. Proc SPIE. 2007; 6770:1–12.
15. Wu MC, Prosser WH. Simultaneous Temperature and Strain Sensing for Cryogenic Applications Using Dual-Wavelength Fiber Bragg Gratings. Proc SPIE. 2003; 5191:208–213.
16. Yeager, CJ.; McGee, C.; Maklad, M.; Swinehart, PR. Cryogenic Fiber Optic Temperature Sensors Based on Fiber Bragg Gratings. Advances in cryogenic engineering: Transactions of the Cryogenic Engineering Conference-CEC; AIP Conference Proceedings; 2006. p. 267-272.
17. Swinehart, PR.; Maklad, M.; Courts, SS. Cryogenic Fiber Optic Sensors Based on Fiber Bragg Gratings. CEC-ICMC Conference Proceedings; 2007. p. 16-20.
18. Huber R, Wojtkowski M, Fujimoto JG. Fourier domain mode locking (FDML): A new laser operating regime and applications for optical coherence tomography. Opt Express. 2006; 14:3225–3237. [PubMed: 19516464]
19. Huber R, Adler DC, Fujimoto JG. Buffered Fourier domain mode locking: unidirectional swept laser sources for optical coherence tomography imaging at 370,000 lines/s. Opt Lett. 2006; 31:2975–2977. [PubMed: 17001371]
20. Adler DC, Huber R, Fujimoto JG. Phase-sensitive optical coherence tomography at up to 370,000 lines per second using buffered Fourier domain mode-locked lasers. Opt Lett. 2007; 32:626–628. [PubMed: 17308582]
21. Jeon MY, Zhang J, Wang Q, Chen Z. High-speed and wide bandwidth Fourier domain mode-locked wavelength swept laser with multiple SOAs. Opt Express. 2008; 16:2547–2554. [PubMed: 18542336]
22. Kranendonk LA, Huber R, Fujimoto JG, Sanders ST. Wavelength-agile $H_2O$ absorption spectrometer for thermometry of general combustion gases. Proc Combust Inst. 2007; 31:783–790.
23. Yun SH, Boudoux C, Pierce MC, de Boer JF, Tearney GJ, Bouma BE. Extended-cavity semiconductor wavelength-swept laser for biomedical imaging. IEEE Photon Technol Lett. 2006; 16:293–295.
24. Huber R, Wojtkowski M, Taira K, Fujimoto JG. Amplified, frequency swept lasers for frequency domain reflectometry and OCT imaging: design and scaling principles. Opt Express. 2005; 13:3513–3528. [PubMed: 19495256]
25. Gagliardi G, Salza M, Ferraro P, De Natale P. Fiber Bragg-grating strain sensor interrogation using laser radio-frequency modulation. Opt Express. 2005; 13:2377–2384. [PubMed: 19495128]

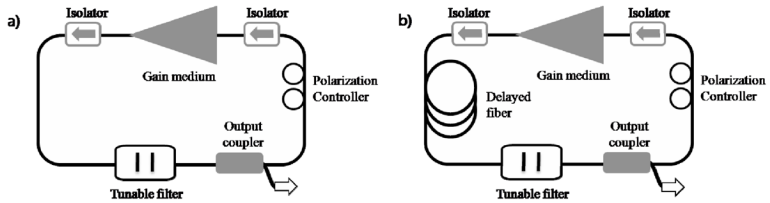


**Fig. 1.**
Schematic of (a) conventional wavelength swept laser and (b) FDML wavelength swept laser, which included a delayed fiber.

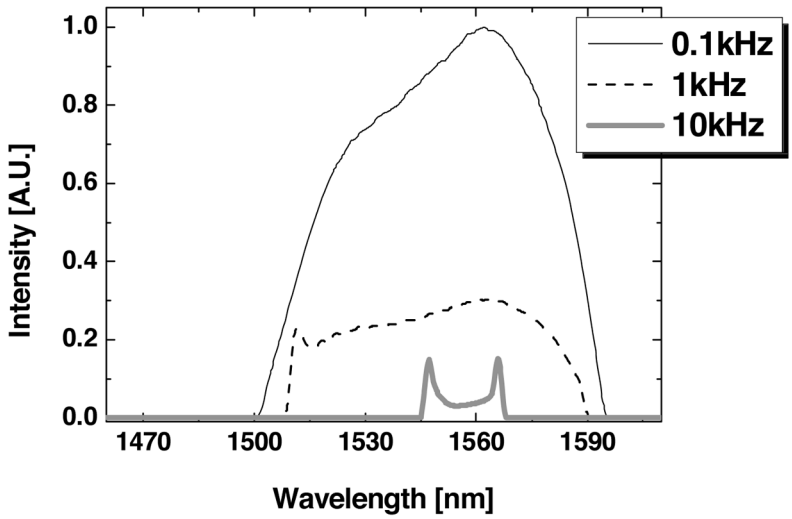


**Fig. 2.**
Spectra of the conventional wavelength swept laser source at different sweeping rates.

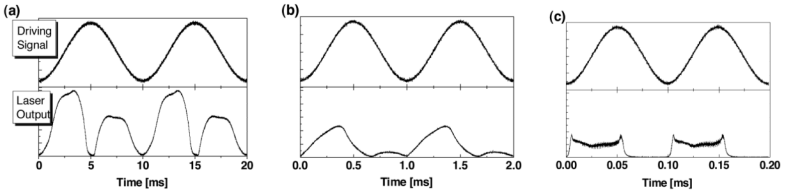


**Fig. 3.**

Temporal transient intensity profiles of the conventional wavelength swept laser source at sweeping rates of (a) 0.1 kHz, (b) 1 kHz and (c) 10 kHz.

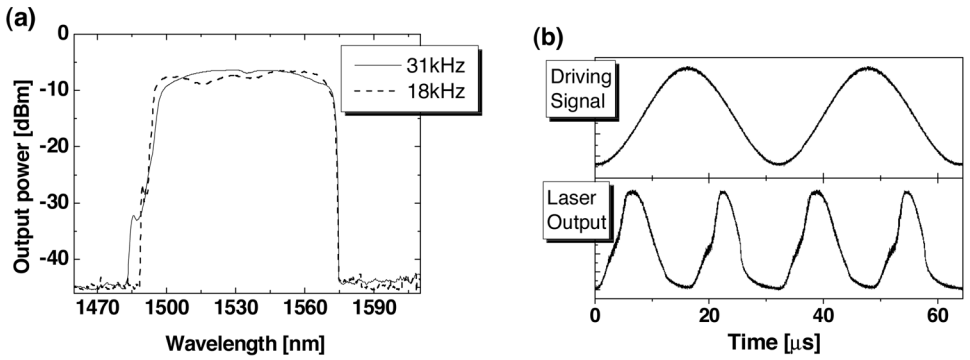


**Fig. 4.**

(a) Integrated output spectra (b) Temporal transient intensity profiles of the FDML wavelength swept laser source at 31.3 kHz.

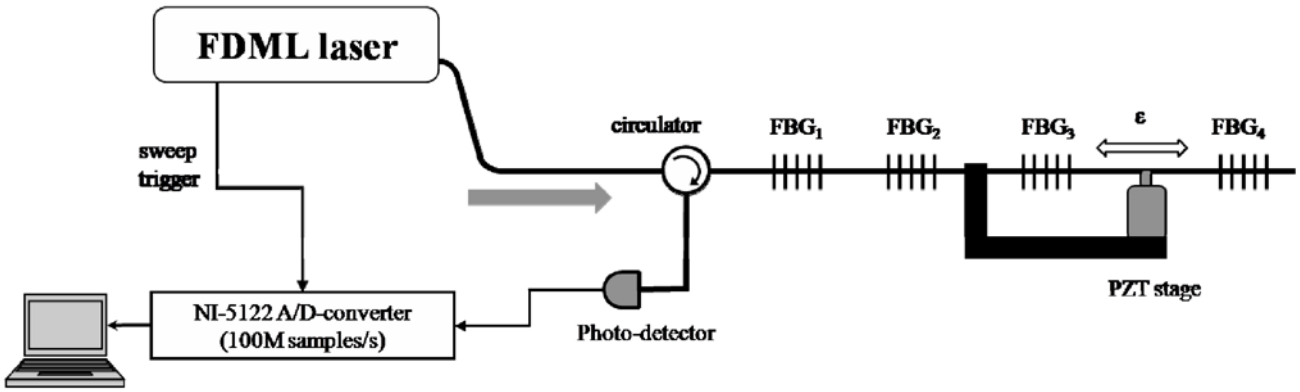


**Fig. 5.**
Experimental set-up for the FBG sensor interrogation system based on a FDML wavelength swept laser.

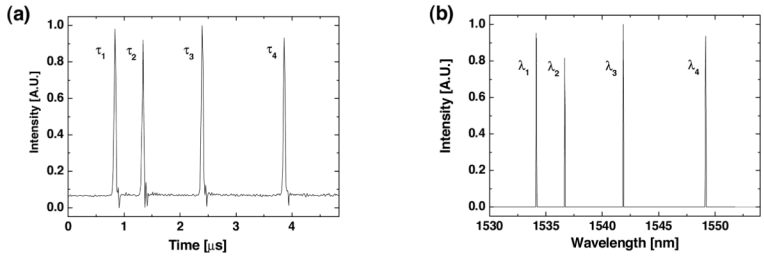


**Fig. 6.**

Experimental measurements of the reflection spectrum of sensors array in (a) the time-domain using a FDML wavelength swept laser and a single detector and (b) the wavelength-domain using a broadband light source and an OSA.

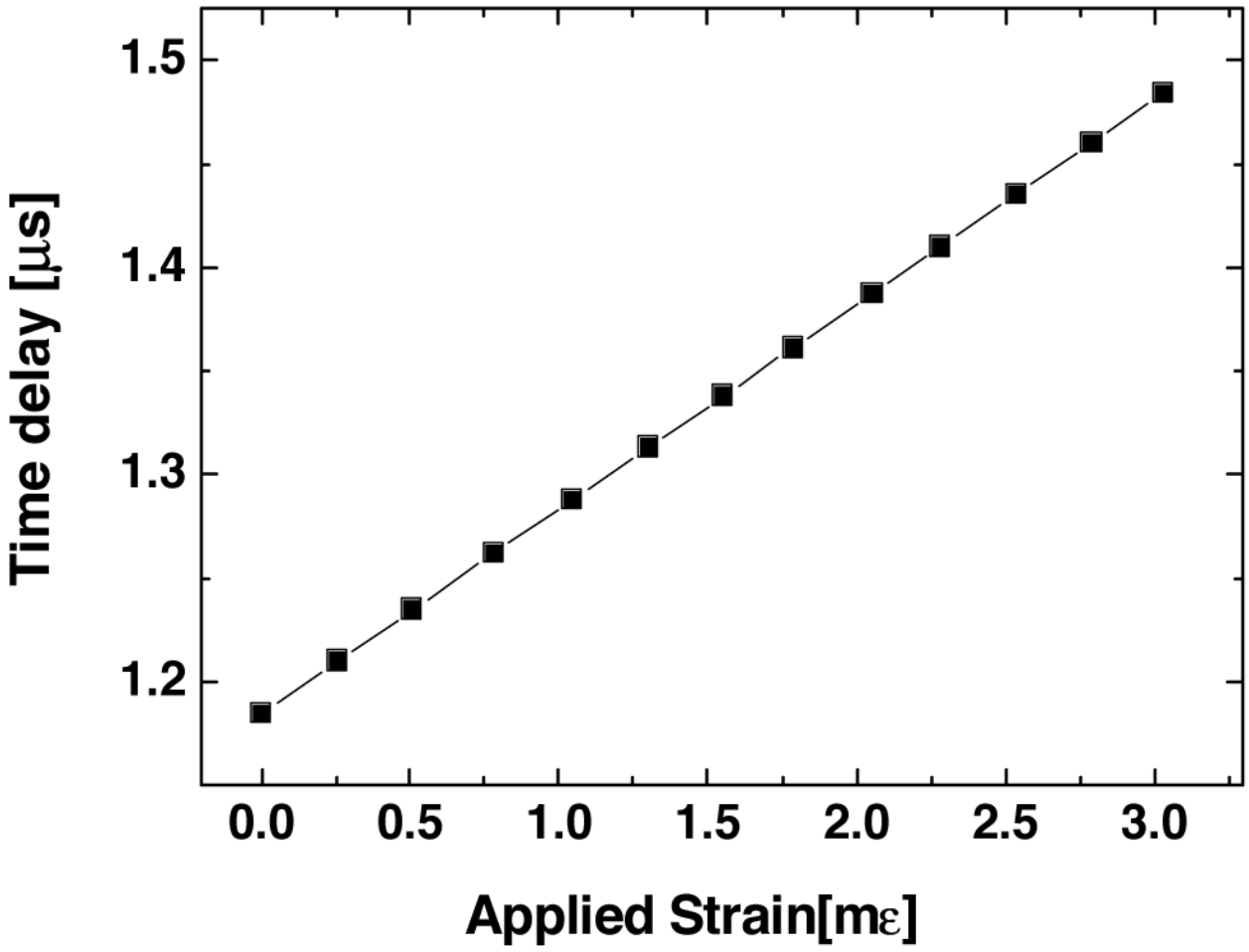


**Fig. 7.**
Plot of the time delay (τ3-τ2) as a function of applied static strain.

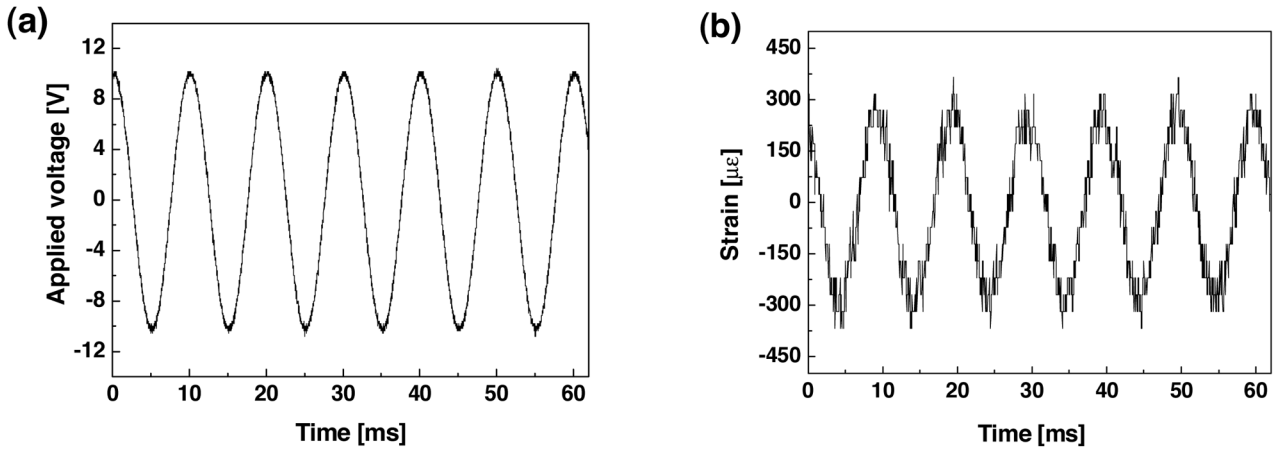


**Fig. 8.**

(a) Input signal to the PZT actuator. (b) Time response of peak points from grating τ3 using the FDML wavelength swept laser at a 31.3 kHz sweep rate.

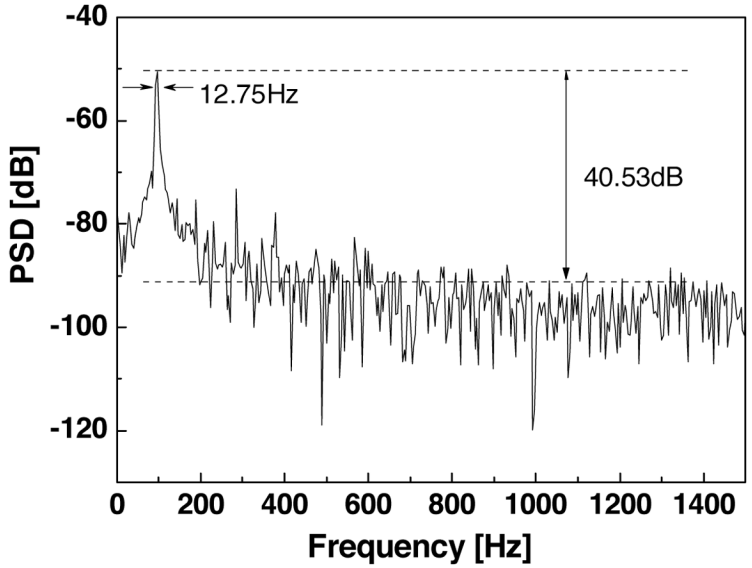


**Fig. 9.**
PSD FFT spectrum of the time-interval measurement data for a 100 Hz dynamic strain.